Proceedings of the
47th IEEE Conference on Decision and Control
Cancun, Mexico, Dec. 9-11, 2008

Cooperative Control of an Autonomous Sampling Network in an External Flow Field

Derek A. Paley

Abstract— **Cooperative steering controls enable mobile sampling platforms to conduct synoptic, adaptive surveys of dynamic spatiotemporal processes by appropriately regulating the space-time separation of their sampling trajectories. Sensing platforms in the air and sea are often pushed off course by strong and variable flow fields such as atmospheric winds and ocean currents. However, many existing cooperative control algorithms are based on simple motion models that do not include a drift vector field. In this paper, we describe a planar motion model that explicitly incorporates a uniform and constant flow field. We also provide decentralized control algorithms that stabilize circular motion, in which all of the particles travel around a circle with a fixed center, and time-splay circular motion, in which the vehicle velocities are synchronized modulo a constant time delay. The proposed time-splay circular formation algorithm—a composition of the circular formation algorithm and a delay differential equation on the N-torus—generates a set of vehicle trajectories that collectively sample each point on the circle at a regular interval.**

I. INTRODUCTION

Autonomous vehicles provide a robust sensing platform for synoptic and adaptive sampling of spatiotemporal processes in the air and sea. Decentralized control algorithms that coordinate the sampling trajectories of multiple vehicles enhance the sensory performance of the entire fleet by appropriately regulating the space-time separation of sample points [1]. A major impediment to the regulation of trajectory separation is the presence of an external flow field—e.g., ocean currents and atmospheric winds. Cooperative control algorithms that are effective in weak flow fields often fail in moderate to strong flows. In this paper, we provide control algorithms suitable for a moderate flow field that is constant in time and uniform in space. (We assume that the flow field is known.) The extension to strong and variable flows is the subject of ongoing work.

Robust coordination of multiple vehicles in the absence of flow can be produced by cooperative control of a dynamic motion model in which each vehicle is represented by a Newtonian particle moving at constant speed in a plane [2], [3], [4]. Each particle is subject to a gyroscopic (steering) control that determines the rate of rotation of the particle velocity. Using the particle framework, theoretically justified algorithms provided in [5], [6] generate symmetric formations in which the relative distance and relative orientation of all vehicles is optimized for sampling performance—under very mild assumptions on the inter-vehicle communication. These algorithms have been successfully demonstrated in multiple at-sea experiments with autonomous underwater vehicles [7], [8].

Analysis of ocean-sampling field experiments highlights the need to develop theoretically justified algorithms that stabilize collective motion in the presence of a strong and variable flow field [9, Chapter 9]. Underwater vehicles routinely encounter ocean currents that match or exceed vehicle speed. These currents push vehicles away from their desired trajectories and compress/expand the space-time separation of multiple trajectories—leading to a degradation of overall sampling performance. Strong currents that vary substantially in time are especially challenging because of the inherent uncertainty in current forecasts. The derivation of cooperative control and estimation algorithms for strong and variable currents is beyond the scope of this paper.

In this paper, we describe a planar particle model that explicitly incorporates a known, uniform and constant flow field whose magnitude does not exceed the particle speed. We provide decentralized control algorithms that stabilize circular motion, in which all of the particles travel around a circle with a fixed center, and time-splay circular motion, in which the vehicle velocities are synchronized modulo a constant time delay. The proposed time-splay circular formation algorithm—a composition of the circular formation algorithm and a delay differential equation on the N-torus—generates a set of vehicle trajectories that collectively sample each point on the circle at a regular interval. Algorithms that stabilize synchronized and balanced trajectories are provided in [10]. These motion primitives collectively form a foundation upon which more complex mission-specific trajectories can be constructed.

The results presented here contribute to a growing literature on motion-planning strategies for unmanned vehicles in an external field [11], [12], [13], [14]. The problem of stabilizing a formation of current- or wind-aided vehicles around an inertially-fixed point very closely resembles the problem of using a vehicle formation to orbit a moving target; the latter problem is studied in [15], [16], [17], [18], [19]. In [17, Chapter 5], the notion of a time-splay configuration is introduced in the context of a sliding-mode solution to the target-tracking problem in which vehicles orbit the target at regular intervals. We further explore the time-splay notion, utilizing in our control design concepts from the literature on phase oscillators with time-delayed coupling [20], [21], [22], [23].

The paper has the following outline. In Section II we describe a self-propelled particle model that explicitly incorporates an external flow field. In Section III we provide decen-

D. Paley is with the Department of Aerospace Engineering, University of Maryland, College Park, MD 20742, USA dpaley@umd.edu

978-1-4244-3124-3/08/$25.00 ©2008 IEEE

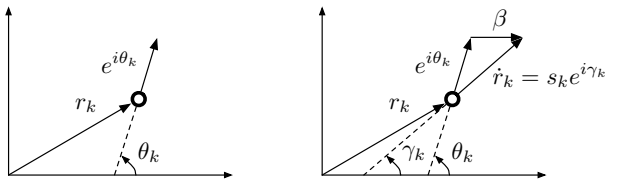

(a) Without flow (b) With flow β

Fig. 1. Coordinates and notation for self-propelled particle model.

tralized control algorithms to stabilize circular formations in the presence of a uniform and constant flow. We also propose a time-splay circular formation algorithm that regulates the temporal spacing of particles in the formation. In Section IV, we summarize the results and provide indications of ongoing and future work.

II. MODEL

Previous work on cooperative control of autonomous vehicles has focused on a self-propelled particle model in which N point masses move at unit speed in an inertial plane [2], [3], [4], [5], [6]. In this model, the position of the kth particle is denoted by r_k, where $k \in \{1,\dots,N\}$, and the velocity of the kth particle is denoted by $\dot{r}_k$.[1] In complex notation, the velocity is $\dot{r}_k = e^{i\theta_k}$, where $\theta_k \in S^1$ describes the orientation of the velocity. Each particle is subject to a state-feedback control u_k. The particle model is [2]

$$\begin{aligned} \dot{r}_k &= e^{i\theta_k} \\ \dot{\theta}_k &= u_k. \end{aligned} \tag{1}$$

The model (3) is illustrated in Figure 1(a).

Motivated by field experiments in operationally challenging environments, it is natural to explicitly incorporate a flow field in the particle model (1) by introducing a flow field $f_k \in \mathbb{C}$. With flow, the particle model (1) becomes

$$\begin{aligned} \dot{r}_k &= f_k + e^{i\theta_k} \\ \dot{\theta}_k &= u_k. \end{aligned} \tag{2}$$

In general, the flow f_k may vary in time and space, i.e. $f_k = f_k(t)$ and $f_k \neq f_j$. Furthermore, it is likely that the actual flow is unknown and, therefore, should not be used for path planning. In this case, one might replace f_k in (2) with $\hat{f}_k$, an estimate of the flow—an approach not pursued here.

Following [10], we study a special case of (2) in which the flow is uniform in space and constant in time. We assume that the magnitude of the flow is less than one (the particle speed). Without loss of generality, we align the positive real axis of an inertial reference frame (i.e., an earth-fixed frame) with the orientation of the flow. Let $\beta \in \mathbb{R}$ denote the magnitude of the flow in the inertial frame, where $|\beta| < 1$. The particle model (2) becomes

$$\begin{aligned} \dot{r}_k &= \beta + e^{i\theta_k} \\ \dot{\theta}_k &= u_k. \end{aligned} \tag{3}$$

[1] A few words about the notation used in this paper: We drop the subscript and use bold to represent an $N \times 1$ matrix, e.g, $r \triangleq [r_1 \cdots r_N]^T$. We identify the $\mathbb{R}^2$ plane with the complex $\mathbb{C}$ plane to facilitate our analysis. The inner product in $\mathbb{R}^2$ is represented in $\mathbb{C}$ by $\langle x,y\rangle = \mathrm{Re}\{\bar{x}y\}$, where $x,y \in \mathbb{C}$ and $\bar{x}$ denotes the complex conjugate of x.

Model (3) is illustrated in Figure 1(b).

To simplify (3), let $s_k \in \mathbb{R}$ and $\gamma_k \in S^1$ denote, respectively, the magnitude and orientation of the inertial velocity, $\dot{r}_k$, i.e., $s_k e^{i\gamma_k} = \beta + e^{i\theta_k}$. Since, by assumption, $|\beta| < 1$, we observe that $s_k > 0$. We calculate

$$\begin{aligned} s_k &= \sqrt{(\beta + e^{i\theta_k})(\beta + e^{-i\theta_k})} \\ &= \sqrt{1 + \beta^2 + 2\beta\cos\theta_k}. \end{aligned} \tag{4}$$

However, we would like to express s_k in terms of γ_k instead of θ_k. Using Figure 1(b), we observe that

$$\sin\theta_k = s_k \sin\gamma_k \tag{5}$$

$$\cos\theta_k = s_k \cos\gamma_k - \beta. \tag{6}$$

Substituting (6) into (4) and rearranging the result yields a quadratic equation in s_k,

$$s_k^2 - 2\beta\cos\gamma_k s_k + \beta^2 - 1,$$

which has the solution (using the positive root, since $s_k > 0$)

$$s_k = \beta\cos\gamma_k + \sqrt{1 - \beta^2\sin^2\gamma_k}. \tag{7}$$

The orientation γ_k is defined as

$$\gamma_k = \arg\{\beta + \cos\theta_k + i\sin\theta_k\} = \mathrm{atan}\left(\frac{\sin\theta_k}{\beta + \cos\theta_k}\right).$$

Differentiating with respect to time the expression

$$\tan\gamma_k = \frac{\sin\theta_k}{\beta + \cos\theta_k}$$

and solving for $\dot{\gamma}_k$, we obtain

$$\dot{\gamma}_k = (\sin^2\gamma_k + \cos\gamma_k \sin\gamma_k \cot\theta_k) u_k. \tag{8}$$

Substituting (5) and (6) into (8) yields

$$\dot{\gamma}_k = (1 - \beta s_k^{-1}\cos\gamma_k) u_k \triangleq \nu_k. \tag{9}$$

We view $\nu_k \in \mathbb{R}$ as a control input, since given ν_k, we can solve for u_k and integrate the model (3). The model (3) becomes [10]

$$\begin{aligned} \dot{r}_k &= s_k e^{i\gamma_k} \\ \dot{\gamma}_k &= \nu_k, \end{aligned} \tag{10}$$

where $s_k = s_k(\gamma_k)$ is defined in (7). We use the particle model (10) in the design of our feedback control algorithms. It represents a self-propelled particle model in which the particle speed depends on the orientation of its velocity.

III. RESULTS

A. Circular Formation Control

In the absence of flow, i.e., using the model (1), setting u_k equal to a constant $\omega_0 \neq 0$ drives particle k around a circle of radius ω_0^{-1} and fixed center, c_k, given by [5]

$$c_k \triangleq r_k + \omega_0^{-1} i \frac{\dot{r}_k}{|\dot{r}_k|}. \tag{11}$$

In the presence of uniform and constant flow, we have the following result [10].

Lemma 1: The model (10) with flow speed $|\beta| < 1$ and the control

$$\nu_k = \omega_0 s_k \tag{12}$$

drives particle k around a circle of radius ω_0^{-1} centered at $c_k(t) = r_k(0) + \omega_0^{-1} i e^{i\gamma_k(0)}$.

Proof: We derive the control ν_k that steers the particle around a circle of radius ω_0^{-1} by differentiating (11) along solutions of (10). This results in

$$\dot{c}_k = s_k e^{i\gamma_k} - \omega_0^{-1} e^{i\gamma_k} \nu_k = (s_k - \omega_0^{-1}\nu_k) e^{i\gamma_k}. \tag{13}$$

Substituting (12) into (13) yields $\dot{c}_k = 0$, which completes the proof. ■

A *circular formation* is a solution of the particle model (10) in which all of the particles orbit the same circle in the same direction [2]. In a circular formation, $c_k = c_j$ for all pairs j and k, which implies that a circular formation satisfies the condition $P\mathbf{c} = 0$ [5], where

$$P = \mathrm{diag}\{\mathbf{1}\} - \frac{1}{N}\mathbf{1}\mathbf{1}^T \tag{14}$$

projects $\mathbb{C}^N$ to the subspace complementary to the span of $\mathbf{1} \triangleq [1 \cdots 1]^T \in \mathbb{R}^N$.

We derive a decentralized control that stabilizes a circular formation by considering the potential [5]

$$S(r, \gamma) \triangleq \frac{1}{2}\langle \mathbf{c}, P\mathbf{c} \rangle. \tag{15}$$

Note $S \geq 0$, with equality only when $\mathbf{c} = c_0\mathbf{1}$, $c_0 \in \mathbb{C}$. The time derivative of S along solutions of (10) is

$$\dot{S} = \sum_{j=1}^{N} \langle \dot{c}_j, P_j\mathbf{c} \rangle = \sum_{j=1}^{N} \langle e^{i\gamma_j}, P_j\mathbf{c} \rangle (s_j - \omega_0^{-1}\nu_j), \tag{16}$$

where P_k denotes the kth row of P. The following result provides a control algorithm to stabilize a circular formation in a uniform and constant flow [10]. It extends [5, Theorem 2], which provides a circular-formation algorithm for the flow-less model (1).

Theorem 1: All solutions of the particle model (10) with flow speed $|\beta| < 1$ and the control

$$\nu_k = \omega_0 (s_k + K\langle P_k\mathbf{c}, e^{i\gamma_k} \rangle),\ K > 0, \tag{17}$$

converge to a circular formation with radius ω_0^{-1} and direction determined by the sign of ω_0.

Proof: The potential S is positive definite and proper in the space of relative circle centers. Substituting (17) into (16) yields

$$\dot{S} = -K \sum_{j=1}^{N} \langle P_k\mathbf{c}, e^{i\gamma_j} \rangle^2 \leq 0.$$

By the invariance principle, all of the solutions of (10) with control (17) converge to the largest invariant set, Λ, in which

$$\langle P_k\mathbf{c}, e^{i\gamma_k} \rangle \equiv 0. \tag{18}$$

In this set, $\dot{\gamma}_k = \omega_0 s_k$ and $\dot{c}_k = 0$. Therefore, in order to satisfy the invariance condition, (18), all of the solutions in Λ must satisfy $P\mathbf{c} = 0$, which is the circular-formation condition. Application of Lemma 1 completes the proof. ■

We illustrate Theorem 1 in Figure 2(a), for $N = 15$, $\beta = 0.75$, $K = 0.01$, and $\omega_0 = 0.1$.

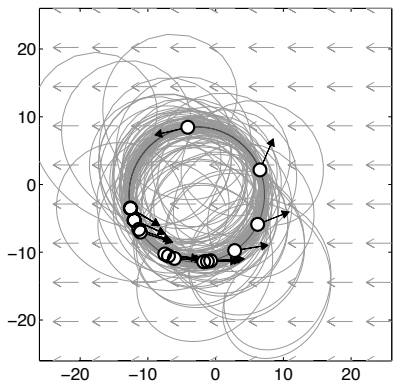

(a) Translation-invariant control

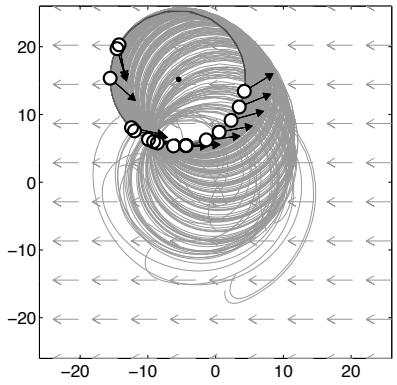

(b) Symmetry-breaking control

Fig. 2. Stabilization of circular motion with $N = 15$, $\omega_0 = 0.01$, and flow speed $\beta = -0.75$. (a) Under the control (17) with $K = 0.01$, the particles converge to a circular formation with an arbitrary center. (a) Under the control symmetry-breaking control (21) with $K = 0.01$, the particles converge to a circular formation with center equal to the reference point $c_0 = -5.46 + i15.19$ (indicated by black dot).

B. Symmetry Breaking Control

The control algorithm described in Theorem 1 depends only on relative positions, i.e., $r_k - r_j$, for any pair k and j. Consequently, it preserves a symmetry of the closed-loop particle model (10) that renders it invariant to rigid translation of the collective [2]. This property of the control algorithm implies the steady-state center of the circle depends only on initial conditions. For applications in path-planning [1] and target tracking [18], [19], there exists the need to specify the steady-state center of the vehicle formation in the presence of flow. We describe a symmetry-breaking algorithm that provides this capability [10].

Following [6], we introduce a virtual particle $k = 0$ that serves as a reference. The virtual particle dynamics,

$$\begin{aligned} \dot{r}_0 &= s_0 e^{i\gamma_0} \\ \dot{\gamma}_0 &= \omega_0 s_0, \end{aligned} \tag{19}$$

where $\omega_0 \neq 0$, are independent of the dynamics of the particles; they drive particle 0 in a circle with fixed center

$c_0 = r_0(0) + \omega_0^{-1} i e^{i\gamma_0(0)}$. The virtual-particle states are available to a subset of the particles, called informed particles. Let $a_{k0} = 1$ if particle k is an informed particle and $a_{k0} = 0$ otherwise.

Consider augmenting the potential S defined in (15) with the quadratic potential [6]

$$S_0 = \frac{1}{2} \sum_{j=1}^{N} a_{j0} |c_j - c_0|^2,$$

which is minimized when $c_j = c_0$ for all $\{j \mid j \in 1,\ldots,N,\ a_{j0} = 1\}$. The time-derivative of $\tilde{S} \triangleq S + S_0$ along solutions of (10) is

$$\dot{\tilde{S}} = \sum_{j=1}^{N} \left(\langle e^{i\gamma_j}, P_j \mathbf{c} \rangle + a_{j0} \langle e^{i\gamma_j}, c_j - c_0 \rangle \right) (s_j - \omega_0^{-1} \nu_j) \quad (20)$$

This leads to the following result [10], which is illustrated in Figure 2(b).

Corollary 1: Let $c_0 = r_0(0) + \omega_0^{-1} i e^{i\gamma_0(0)}$ be the fixed reference provided by the virtual particle $k = 0$ with dynamics (19). Let a_{k0}, $k = 1,\ldots,N$, equal one if particle k is informed of this reference and zero otherwise. If there is at least one informed particle and no more than $N-1$ informed particles, then all solutions of the particle model (10) with the control

$$\nu_k = \omega_0 (s_k + K(\langle e^{i\gamma_k}, P_k \mathbf{c} \rangle + a_{k0} \langle e^{i\gamma_k}, c_k - c_0 \rangle)),\ K > 0, \quad (21)$$

converge to a circular formation with radius ω_0^{-1}, direction determined by the sign of ω_0, and center c_0.

Proof: With the control (21), the time-derivative of the augmented potential $\tilde{S}$ satisfies

$$\dot{\tilde{S}} = -K \sum_{j=1}^{N} (\langle e^{i\gamma_j}, P_j \mathbf{c} \rangle + a_{j0} \langle e^{i\gamma_j}, c_j - c_0 \rangle)^2 \leq 0.$$

By the invariance principle, all solutions converge to the largest invariant set, Λ, for which

$$\langle e^{i\gamma_k}, P_k \mathbf{c} \rangle + a_{k0} \langle e^{i\gamma_k}, c_k - c_0 \rangle \equiv 0 \quad (22)$$

for $k = 1,\ldots,N$. In this set, $\dot{\gamma}_k = \omega_0 s_k$ and $\dot{c}_k = 0$. For $a_{k0} = 0$, then the invariance condition (22) is satisfied only if $P_k \mathbf{c} = 0$. This implies $\mathbf{c}$ is in the span of $\mathbf{1}$, i.e. $c_k = c_j$ for all pairs k and j. For $a_{k0} = 1$, the invariance condition becomes

$$\langle e^{i\gamma_k}, c_k - c_0 \rangle \equiv 0,$$

which holds only if $c_k = c_0$. This implies $\mathbf{c} = c_0 \mathbf{1}$, which completes the proof. ∎

C. Time-Splay Circular Formation Control

Both algorithms presented thus far stabilize circular formations with arbitrary spacing of particles along the circle. In sensing applications, it is often of interest to regulate the spatiotemporal characteristics of sampling trajectories by driving the sensing platforms in symmetric formations [1]. Symmetric circular formations are circular formations in which the particles are arranged in a symmetric pattern that mirrors their phase configuration [5], [6]. For example, the symmetric pattern in which all of the particles are uniformly spaced around the circle is called a *splay* formation, named after the splay phase configuration [24], [25]. In the absence of flow, i.e., for model (1), symmetric circular formations are generated by combining a circular formation control with a phase control algorithm [5]. In the presence of moderate uniform and constant flow, i.e., for model (10), we also pursue a composite approach to the stabilization of symmetric circular formations, albeit with a different notion of a symmetric phase configuration.

The approach to stabilization of symmetric phase configurations provided in [5], [6] is based on rotationally-invariant gradient controls that either synchronize or balance (i.e., drive the phasor centroid to zero) multiple phase harmonics. For the splay configuration, each phase harmonic is balanced up to the Nth harmonic, which is synchronized. It is possible to perform phase synchronization and balancing in a circular formation because the phase control algorithms are rotationally invariant.

Although phase synchronization and balancing of the model (10) is possible [10], the existence of balanced circular motion is not guaranteed because of the lack of rotational invariance. For example, consider the balanced configuration for $N = 2$, given by $\gamma_1(t) = \gamma_2(t) + \pi$. By Lemma 1, the phase dynamics of a particle orbiting a circle is

$$\dot{\gamma}_k = \omega_0 s_k, \quad (23)$$

where $s_k = s_k(\gamma_k)$ is defined in (7). Along solutions of (23), the quantity $\gamma_1(t) - \gamma_2(t)$ is not conserved for any initial conditions other than synchronization.

For phase oscillators with the dynamics (23), an alternate notion of a balanced phase configuration is to consider the *temporal* phase separation. For $N = 2$, the configuration $\gamma_1(t) = \gamma_2(t - \tau)$, where $\tau > 0$ is a time delay, is preserved under (23). The time-delay τ represents the temporal separation of phases γ_1 and γ_2. Therefore, a quasi-balanced phase configuration is to set $\tau = T/2$, where T is the period of revolution. (We find T by integrating (23) over one revolution. Using separation of variables, we have

$$\int_0^{2\pi} \frac{d\gamma_k}{s_k} = \int_0^T \omega_0 dt = \omega_0 T.$$

Integrating and solving for T yields $T = 4E(\beta)/(\omega_0(1 - \beta^2))$, where $E(\cdot)$ is Legendre's complete elliptic integral of the second kind [26].)

Generally, a *time-splay* configuration is defined as [17, Chapter 5]

$$\begin{aligned} \gamma_k(t) &= \gamma_{k+1}(t - T/N),\ k = 1,\ldots,N-1, \\ \gamma_N(t) &= \gamma_1(t - T/N), \end{aligned} \quad (24)$$

where T is the period of oscillation). The main result of this section is to propose a control algorithm that stabilizes the set of time-splay phase configurations. This algorithm, when combined with a circular formation algorithm, yields a time-splay circular formation in a uniform and constant flow (see Figure 3(a)).

Consider the closed-loop phase model

$$\begin{aligned} \dot{\gamma}_k &= \omega_0 s_k + K \sin(\gamma_{k+1}(t - \tau) - \gamma_k),\ k = 1,\ldots,N-1, \\ \dot{\gamma}_N &= \omega_0 s_N + K \sin(\gamma_1(t - \tau) - \gamma_N), \end{aligned} \quad (25)$$

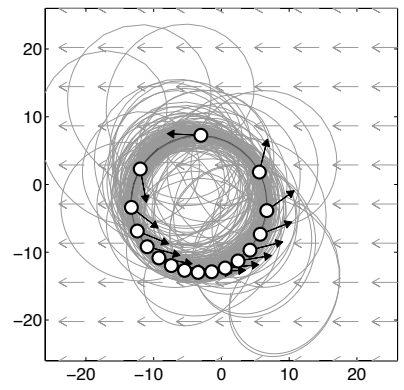

(a) Composite control

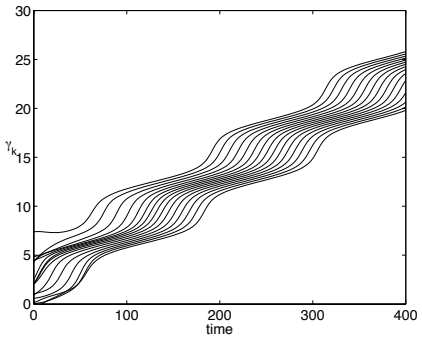

(b) Time-splay stabilization

Fig. 3. Stabilization of time-splay circular motion with $N = 15$, $\omega_0 = 0.1$, and flow speed $\beta = -0.75$. (a) Under the composite control (33) with $K_0 = K_1 = 0.01$, the particles converge to a timne-splay circular formation. (b) Convergence of the phases γ_k, $k = 1,\ldots,N$, to a time-splay phase configuration.

where $\tau \triangleq T/N$, $K > 0$, and $\gamma_k(t) = \gamma_k(0)$, for all $t < 0$. The system (25) is a delay differential equation on the N-torus that sinusoidally couples $\gamma_k(t)$ to $\gamma_{j(k)}(t-\tau)$ over a directed-ring topology, i.e., $j(k) = k \bmod N+1$. The goal of this coupling is to (locally) synchronize $\gamma_k(t)$ with a time-delayed representation of $\gamma_{j(k)}(t)$, i.e., $\gamma_{j(k)}(t-\tau)$. Time-delayed sinusoidal coupling over an undirected graph is known to locally synchronize $\gamma_k(t)$ and $\gamma_{j(k)}(t)$ [21], [22]; however, we are not aware of any previous examination of the stability of the time-splay phase configuration over a directed ring.

In order to examine the stability of the time-splay phase-configuration, let $\gamma(t)$ represent a solution to the uncoupled system (23). We are concerned with the stability of periodic solutions to (25) of the form

$$\begin{aligned} \gamma_1(t) &= \gamma(t-\delta) + \phi_1(t) \\ \gamma_k(t-(k-1)\tau) &= \gamma(t-\delta) + \phi_k(t-(k-1)\tau),\ k = 2,\ldots,N, \end{aligned} \tag{26}$$

where $\delta \geq 0$ is an unknown time lag. The ϕ_k variables represent angular displacements from the periodic solution γ. (When $\phi_k(t) = 0$, $k = 1,\ldots,N$, the phase configuration γ is time-splayed.) The time-lag δ is independent of k. (We need to include δ because of the lack of rotational symmetry of the system (25).)

We determine the dynamics of ϕ by time-differentiating (26) along solutions of (23) and (23), which yields the non-autonomous delay differential equation

$$\begin{aligned} \dot{\phi}_k &= \omega_0(s_k(\gamma(t-\delta)+\phi_k) - s_k(\gamma(t-\delta)) + \\ &\quad K\sin(\phi_{j(k)}(t-\tau) - \phi_k),\ k = 1,\ldots,N. \end{aligned} \tag{27}$$

To first order, the dynamics (27) are

$$\dot{\phi}_k = \xi(t)\phi_k + K(\phi_{j(k)}(t-\tau) - \phi_k), \tag{28}$$

where $\xi(t) = \omega_0 \left.\frac{\partial s_k}{\partial \gamma_k}\right|_{\gamma(t-\delta)}$ is odd and T-periodic. (It is also straightforward to show that $|\xi(t)| \leq 2|\omega_0|$ for all t, although that fact is not used here.)

Following [21], we evaluate the stability of (28) by considering solutions of the form $\phi_k(t) = \rho_k e^{\lambda t}$. The eigenvalues of (28) are the roots of

$$\rho_k \lambda e^{\lambda t} = \xi(t)\rho_k e^{\lambda t} + K(s_{j(k)} e^{\lambda(t-\tau)} - \rho_k e^{\lambda t}). \tag{29}$$

Rearranging (29) yields [21]

$$As = \sigma s, \tag{30}$$

where $s = (s_1,\ldots,s_N)^T$, A is the adjacency matrix of a directed ring graph with N nodes, and σ is an eigenvalue of A given by

$$\sigma = \frac{e^{\lambda\tau}}{K}(\lambda + K - \xi(t)). \tag{31}$$

Note, A is an $N \times N$ circulant matrix whose first row is $(0,1,0,\ldots,0) \in \mathbb{R}^N$. As observed in [21], we conclude from the Gersgorin circle theorem that $|\sigma| \leq 1$ since the diagonal entries of A are zero and the deleted absolute row sums of A are equal to one. Letting $\sigma = |\sigma|e^{i\alpha}$, we rearrange (31) to obtain

$$|\sigma| K e^{i\alpha} = e^{\lambda\tau}(\lambda + K - \xi(t)), \tag{32}$$

which enables us obtain the following result by applying [21, Proposition 1].

Lemma 2: For $\beta = 0$, the time-splay phase configuration defined in (24) is an exponentially stable equilibrium point of (25) in the reduced space of relative phases.

Proof: This result is a direct consequence of [21, Proposition 1]. When $\beta = 0$, then $s_k = 1$ and $\xi(t) = 0$, in which case (28) becomes an autonomous linear delay differential equation. According to [21, Proposition], equation (28) with $\xi(t) = 0$ and $|\sigma| \leq 1$ implies that $\mathrm{Re}(\lambda) \leq 0$ and the multiplicity of zero as an eigenvalue is one. The zero eigenvalue is associated to the rotational symmetry of the model (25) with $\xi(t) = 0$; the real part of every eigenvalue other than zero is strictly negative. ■

As a consequence of Lemma 2, the time-splay phase configuration (24) is a locally asymptotically stable set of the closed loop model (25) with $\beta = 0$, i.e., with no flow. Simulations strongly suggest that the set of time-splay configurations is asymptotically stable for any $|\beta| < 1$. Analysis of this case is complicated by the fact that the first-order dynamics (27) are non-autonomous, which implies

that its spectral properties alone are insufficient to determine stability. Therefore, the stability analysis of the nonlinear delay differential equation (25) with $|\beta| < 1$ is the subject of ongoing work. The objective of this ongoing work is to determine a Lyapunov functional that, when combined with the circular-formation potential in Section III-A, supports the following proposition. (An alternate version of Proposition 1 is proven in [27].)

Proposition 1: Consider the composite control algorithm

$$v_k = \omega_0(s_k + K_0\langle P_k\mathbf{c}, e^{i\gamma_k}\rangle) + K_1\sin(\gamma_{j(k)}(t-\tau) - \gamma_k), \quad (33)$$

where $K_0 > 0$, $K_1 > 0$, $\gamma_k(t) = \gamma_k(0)$, for all $t < 0$, and $j = k \bmod N+1$. (P_k is the kth row of the matrix, P, defined in 14.) All solutions of the particle model (10) with flow speed $|\beta| < 1$ and the control (33) converge to a circular formation with radius ω_0^{-1} and direction determined by the sign of ω_0. The set of circular formations in which the phases γ are arranged in a time-splay configuration as defined in (24) is asymptotically stable.

A numerical simulation of Proposition 1 is illustrated in Figure 3. In Figure 3(a), the particles bunch together when they slow down and spread out when they speed up. In Figure 3(b), the particle phases achieve the time-splay configuration by synchronizing modulo the time-delay T/N.

IV. CONCLUSIONS

Distributed sensing with multiple, mobile platforms requires cooperative-control algorithms that generate coordinated sampling trajectories in the presence of strong and variable flow fields. The design of these algorithms is based on simple models of platform motion that often ignore the presence of flow. In this paper, we describe a self-propelled particle model that explicitly incorporates the presence of a uniform and constant flow field. We provide a decentralized control algorithm that stabilize circular formations. We also propose a time-delay control that stabilizes the set of circular formations in which the temporal-separation between particle trajectories is uniform. These motion primitives will be essential in constructing a cooperative-control framework for autonomous and distributed sensing in the presence of flow.

REFERENCES

[1] N. E. Leonard, D. A. Paley, F. Lekien, R. Sepulchre, D. M. Fratantoni, and R. E. Davis, "Collective motion, sensor networks and ocean sampling," *Proc. IEEE*, vol. 95, no. 1, pp. 48–74, 2007.

[2] E. W. Justh and P. S. Krishnaprasad, "A simple control law for UAV formation flying," Institute for Systems Research, University of Maryland, Tech. Rep. 2002-38, 2002. [Online]. Available: http://techreports.isr.umd.edu/reports/2002/TR_2002-38.pdf

[3] ——, "Equilibria and steering laws for planar formations," *Systems and Control Letters*, vol. 52, no. 1, pp. 25–38, 2004.

[4] F. Zhang and N. E. Leonard, "Coordinated patterns of unit speed particles on a closed curve," *Systems and Control Letters*, vol. 56, no. 6, pp. 397–407, 2007.

[5] R. Sepulchre, D. A. Paley, and N. E. Leonard, "Stabilization of planar collective motion: All-to-all communication," *IEEE Trans. Automatic Control*, vol. 52, no. 5, pp. 811–824, 2007.

[6] ——, "Stabilization of planar collective motion with limited communication," *IEEE Trans. Automatic Control*, vol. 53, no. 3, pp. 706–719, 2008.

[7] F. Zhang, D. M. Fratantoni, D. A. Paley, J. M. Lund, and N. E. Leonard, "Control of coordinated patterns for ocean sampling," *Int. J. Control*, vol. 80, no. 7, pp. 1186–1199, 2007.

[8] D. A. Paley, F. Zhang, and N. E. Leonard, "Cooperative control for ocean sampling: The Glider Coordinated Control System," *IEEE Trans. Control Systems Technology*, vol. 16, no. 4, pp. 735–744, 2008.

[9] D. A. Paley, "Cooperative control of collective motion for ocean sampling with autonomous vehicles," Ph.D. dissertation, Princeton University, Princeton, New Jersey, September 2007. [Online]. Available: http://wam.umd.edu/ dpaley/papers/paley-thesis.pdf

[10] ——, "Stabilization of Collective Motion in a Uniform and Constant Flow Field," in *Proc. AIAA Guidance, Navigation and Control Conf. and Exhibit*, no. AIAA-2008-7173, Honolulu, Hawaii, August 2008, (8 pages).

[11] N. Ceccarelli, J. J. Enright, E. Frazzoli, S. J. Rasmussen, and C. J. Schumacher, "Micro UAV path planning for reconnaissance in wind," in *Proc. 2007 American Control Conf.*, New York City, New York, July 2007, pp. 5310–5315.

[12] T. G. McGee, S. Spry, and J. K. Hedrick, "Optimal path planning in a constant wind with a bounded turning rate," in *Proc. AIAA Conf. Guidance, Navigation, and Control (electronic)*, no. AIAA 2005-6186, San Francisco, California, August 2005, (11 pages).

[13] T. G. McGee and J. K. Hedrick, "Path planning and control for multiple point surveillance by an unmanned aircraft in wind," in *Proc. 2006 Amer. Control Conf.*, Minneapolis, Minnesota, June 2006, pp. 4261–4266.

[14] R. Rysdyk, "Course and heading changes in significant wind," *J. Guidance, Control, and Dynamics*, vol. 39, no. 4, pp. 1168–1171, 2007.

[15] D. J. Klein and K. A. Morgansen, "Controlled collective motion for trajectory tracking," in *Proc. 2006 American Control Conf.*, Minneapolis, Minnesota, June 2006, pp. 5269–5275.

[16] R. Rysdyk, "Unmanned aerial vehicle path following for target observation in wind," *J. Guidance, Control, and Dynamics*, vol. 29, no. 5, pp. 1092–1100, 2006.

[17] D. B. Kingston, "Decentralized control of multiple UAVs for perimeter and target surveillance," Ph.D. dissertation, Department of Electrical and Computer Engineering, Brigham Young University, Provo, Utah, December 2007. [Online]. Available: http://www.ee.byu.edu/faculty/beard/papers/thesis/DerekKingstonPhD.pdf

[18] E. W. Frew, D. A. Lawrence, and S. Morris, "Coordinated standoff tracking of moving targets using Lyapunov guidance vector fields," *J. Guidance, Control, and Dynamics*, vol. 31, no. 2, pp. 290–306, 2008.

[19] T. H. Summers and M. R. Akella, "Coordinated standoff tracking of moving targets: Control laws and information architectures," in *Proc. AIAA Guidance, Navigation and Control Conf. and Exhibit (electronic)*, no. AIAA-2008-7021, Honolulu, Hawaii, 2008, (25 pages).

[20] E. Klavins and D. E. Koditschek, "Phase regulation of decentralized cyclic robotic systems," *Int. J. Robotics Research*, vol. 21, no. 3, pp. 257–275, 2002.

[21] M. G. Earl and S. H. Strogatz, "Synchronization in oscillator networks with delayed coupling: A stability criterion," *Phys. Rev. E*, vol. 67, no. 3, p. 036204, 2003.

[22] A. Papachristodoulou and A. Jadbabaie, "Synchonization in oscillator networks with heterogeneous delays, switching topologies and nonlinear dynamics," in *Proc. 45th IEEE Conf. Decision and Control*, San Diego, California, 2006, pp. 4307–4312.

[23] N. Chopra and M. Spong, "Passivity-based control of multi-agent systems," in *Advances in Robot Control: From Everyday Physics to Human-Like Movements*, S. Kawamura and M. Svinin, Eds. Springer Verlag, 2006, pp. 107–134.

[24] P. Hadley and M. R. Beasley, "Dynamical states and stability of linear arrays of Josephson junctions," *Appl. Phys. Letters*, vol. 50, no. 10, pp. 621–623, 1987.

[25] D. G. Aronson, M. Golubitsky, and J. Mallet-Paret, "Ponies on a merry-go-round in large arrays of Josephson junctions," *Nonlinearity*, vol. 4, pp. 903–910, 1991.

[26] E. W. Weisstein. Complete elliptic integral of the second kind. From MathWorld–A Wolfram Web Resource. [Online]. Available: http://mathworld.wolfram.com/CompleteEllipticIntegraloftheSecondKind.html

[27] D. A. Paley and C. Peterson, "Stabilization of collective motion in a time-invariant flow field," submitted.